Physica Medica 58 (2019) 114–120

Contents lists available at ScienceDirect

Physica Medica

journal homepage: www.elsevier.com/locate/ejmp

Original paper

The β^- radio-guided surgery: Method to estimate the minimum injectable activity from ex-vivo test

A. Russomando[a,b], M. Schiariti[c,1], V. Bocci[d], M. Colandrea[e], F. Collamati[d,f], M. Cremonesi[g], M.E. Ferrari[h], P. Ferroli[c], F. Ghielmetti[c], R. Ghisini[i], C.M. Grana[e], C. Mancini Terracciano[d], M. Marafini[j,d], R. Mirabelli[a,d], S. Morganti[d], S. Papi[k], M. Patanè[l], G. Pedroli[h], B. Pollo[l], E. Solfaroli Camillocci[a,d,*], G. Traini[a,d], R. Faccini[a,d]

[a] Dip. Fisica, Sapienza Univ. di Roma, Roma, Italy
[b] Centro Cientifico Tecnologico de Valparaso-CCTVal, Universidad Tecnica Federico Santa Maria, Chile
[c] Dip. Neurochirurgia, Fondazione Istituto Neurologico Carlo Besta, Milano, Italy
[d] INFN Sezione di Roma, Roma, Italy
[e] Divisione di Medicina Nucleare, Istituto Europeo di Oncologia, Milano, Italy
[f] Dip. Scienze di Base e Applicate per l'Ingegneria, Sapienza Univ. di Roma, Roma, Italy
[g] Unità Ricerca sulle Radiazioni, Istituto Europeo di Oncologia, Milano, Italy
[h] Servizio Fisica Sanitaria, Istituto Europeo di Oncologia, Milano, Italy
[i] Trial Activation and Reporting - Data Management – Clinical Trial Office Direzione Scientifica, Istituto Europeo di Oncologia, Milano, Italy
[j] Museo Storico della Fisica e Centro Studi e Ricerche "E. Fermi", Roma, Italy
[k] Unità Produzione Radiofarmaci, Istituto Europeo di Oncologia, Milano, Italy
[l] U.O. Anatomia Patologica, Fondazione Istituto Neurologico Carlo Besta, Milano, Italy

ARTICLE INFO

Keywords:
Radio-guided-surgery
Brain tumours
β^- decays
Intraoperative imaging

Purpose: Radio-guided surgery with β^- decays is a novel technique under investigation. One of the main advantages is its capability to detect small ($\leqslant 0.1$ ml) samples after injecting the patient with low activity of radiopharmaceutical. This paper presents an experimental method to quantify this feature based on ex-vivo tests on specimens from meningioma patients.
Methods: Patients were enrolled on the basis of the standard uptake value (SUV) and the tumour-to-non-tumour activity ratio (TNR) resulted from ^{68}Ga-DOTATOC PET exams. After injecting the patients with 93–167 MBq of ^{90}Y-DOTATOC, 26 samples excised during surgery were analyzed with a β^- probe. The radioactivity expected on the neoplastic specimens was estimated according to the SUV found in the PET scan and the correlation with the measured counts was studied. The doses to surgeon and medical personnel were also evaluated.
Results: Even injecting as low as 1.4 MBq/kg of radiotracer, tumour residuals of 0.1 ml can be detected. A negligible dose to the medical personnel was confirmed.
Conclusions: Radio-guided surgery with β^- decays is a feasible technique with a low radiation dose for both personnel and patient, in particular if the patient is injected with the minimum required activity. A correlation greater than 80% was observed between the measured counts and the expected activity for the lesion samples based on the individual SUV and the TNR. This makes identifiable the minimum injectable radiotracer activity for cases where ^{90}Y is the utilized radionuclide.

1. Background

Radio-guided surgery (RGS) is a technique aimed at assisting the surgeon to reach as complete a resection of the tumoural lesion as possible, while minimizing the amount of healthy tissue removed[1]. Before surgery, the patient is administered with a specific radio-labeled tracer which is preferentially absorbed by the tumoural tissue. A probe (for a review see [2]), sensitive to the signal emitted by the radio-tracer, is used to identify the radio-marked tumour lesion. As a result, after the bulk removal, RGS provides the surgeon with real-time information

* Corresponding author at: Dip. Fisica, Univ. di Roma "La Sapienza", I-00185 Rome, Italy.
E-mail address: elena.solfaroli@roma1.infn.it (E. Solfaroli Camillocci).
[1] Co-first-author.

https://doi.org/10.1016/j.ejmp.2019.02.004
Received 30 July 2018; Received in revised form 21 January 2019; Accepted 9 February 2019
Available online 16 February 2019

regarding the presence of small tumoural remnants and affected lymph nodes.

Established methods to date make use of a γ-emitting tracer and either a γ radiation detecting probe[3,4] or a portable gamma camera [5,6]. Since γ radiation can travel through a large amount of tissue, any uptake of the tracer in nearby healthy tissue represents a non-negligible background, limiting and sometimes preventing the use of this technique.

To mitigate this effect it was suggested in literature the use of β^+ decaying tracers. The emitted positrons in fact have a limited penetration and their detection is local. Nonetheless, positrons annihilate with electrons in the body and produce γs with an energy of 511 keV: the background persists and actually increases in energy, forcing the development of dual detectors [7]. As a possible better solution to extend the applicability range of RGS, the use of pure β^--emitting radioisotopes was suggested [8]. β^- radiation, indeed, is characterized by a penetration of only a few millimetres of tissue with essentially no γ contamination, since the Bremsstrahlung contribution, that has a 0.1% emission probability above 100 keV, can be considered negligible [9].

This novel approach allows the developing of a handy and compact probe [10] which, by detecting electrons and operating with low radiation background, provides a clearer delineation of the lesions. As a result, a smaller injected activity is required to detect tumour residuals compared to established RGS approaches. This also implies that the radiation exposure for the medical personnel becomes almost negligible [8].

To explore the applicability of this technique, specific studies have been performed [11,12]. In these studies, a relationship between the activity in tumour or in healthy tissues and the expected signal from the probe was estimated on the basis of a full simulation program (FLUKA [13]). Initially, the clinical cases were limited to the tumours known to express receptors to a β^- emitting radio-tracer, in particular the ^{90}Y-labeled [1,4,7,10-tetraazacyclododecane-N,N′,N″,N‴-tetraacetic acid0-D-Phe1,Tyr3]octreotide (named DOTATOC): meningioma [14] and glioma [15] brain tumours and neuroendocrine tumours (NETs) [16].

To estimate the activity distribution in a real case, the ^{68}Ga-labelled DOTATOC PET images of the patients affected by the clinical pathology of interest were imported in the simulation. Then, the FLUKA program, by simulating all interactions of particles with matter, was able to translate the activity concentrations in the corresponding counting rate that would be recorded by the probe on the same lesion when marked with ^{90}Y-DOTATOC. This relationship was set under the assumption that the bio-distribution of the tracer does not change by substituting the radionuclide. To equalize the simulation forecast to the probe response, the device was characterized with sealed sources and ^{90}Y activated phantoms [10,17]. In all the studied cases (meningioma, glioma and NETs), the radiotracer standard uptake value (SUV) and the tumour-to-non-tumour activity ratios (TNR) from the PET images resulted high enough to allow the detection of 0.1 ml residuals within few seconds of the probe application [11,12,17].

Finally the entire RGS procedure, that start with the evaluation of the SUV in the tumour and the assumption on the bio-distribution in the patient, was validated by ex-vivo measures on meningioma specimens. This also tested the signal detection in a more realistic environment.

This paper reports the results of tests on ex-vivo specimens from patients affected by meningioma as a follow-up of the proof-of-principle published in Ref. [18]. These tests, besides strengthening the evidence obtained from the first patient, aimed at evaluating the minimum detectable activity in meningioma and at establishing a procedure to determine the activity that needs to be administered patient by patient, starting from the SUV estimated with the preoperative PET images.

Table 1
Meningioma patients enrolled in this study: volume (V_T) of the primary lesion estimated with an MRI exam; mean (SUV_{mean}) and standard deviation (SD) of the SUV in the lesion voxels, and TNR evaluated with a ^{68}Ga-DOTATOC PET/CT scan; administered activity (A_{adm}) and total body weight (W). In the last column the activity concentration expected in meningioma at the time of operation (A_{est}) is reported, calculated as defined in the text.

Patient	V_T [ml]	SUV_{mean} [g/ml]	SD(SUV) [g/ml]	TNR	A_{adm} [MBq]	W [kg]	A_{est} [kBq/ml]
1	18.3	4.3	1.1	26	167	104	5.4
2	11.9	3.1	0.9	62	111	77	3.4
3	21.5	2.8	1.2	92	93	65	3.0

2. Methods

2.1. Patient treatment protocol

Meningioma patients were chosen because of the well known high receptivity of this class of tumour to a somatostatin analogue, such as DOTATOC [14].

In addition to the first patient, object of the publication in Ref. [18], three more cases with radiological diagnosis of meningioma were selected for the present study. The three voluntary patients gave written informed consent to participate in the clinical trial (EUDRACT 2013-004033-32) approved by the Ethic Committee (institutional review board) of the *Istituto Neurologico Carlo Besta* and the *Istituto Europeo di Oncologia* of Milan. To assess the *in vivo* presence of somatostatin receptors, a PET/CT scan with ^{68}Ga-DOTATOC was performed about two weeks prior to the surgical intervention. The scan, performed one hour after the injection of 4 MBq/kg of patient weight, allowed the measurement of the mean SUV (SUV_{mean}) and the TNR of the lesions (summarized in Table 1). In all of the cases, the uptake was rated sufficient to test the technique, on the basis of the already published feasibility study [12].

Twenty-four hours before the surgical intervention, the patients were injected with ^{90}Y-DOTATOC. The administered activity (A_{adm} in Table 1) was lowered, case by case, aiming at evaluating the minimum, according to the individual radiotracer uptake (SUV, TNR) and the patient weight, to make a 0.1 ml tumour volume detectable. The estimated activity concentration in meningioma samples at the time of operation was computed as

$$A_{est} = \frac{A_{adm}}{W} * SUV_{mean} * 2^{-\frac{\Delta t}{T_{1/2}}} \quad (1)$$

taking into account the time elapsed from injection (Δt), the patient weight (W), and the ^{90}Y half-time $T_{1/2} = 64$ hr.

It should be noted that the SUV_{mean} was evaluated from the PET scan 1 h after the administration of ^{68}Ga-DOTATOC, while the surgery was performed 24 h after injection of ^{90}Y-DOTATOC. The biodistribution was assumed to be dependent on the drug delivery mechanism and not affected by the labelling radionuclide. Furthermore, a previous study on dose delivery of neuroendocrine patients treated with ^{177}Lu-DOTATOC (see Ref. [12]) observed an increase of the TNR with a maximum after 24 h from the radiotracer administration due to the metabolic washout of the healthy organs. In this study TNR is therefore conservatively underestimated.

After surgery (performed as indicated by the established clinical protocol), the excised tumour volume and the attached dura mater were sectioned in several samples as listed in Tables 2–4. The irregular shape of the samples did not allow a precise measurement of the volume and their textures made the shape itself warp when pushed by the probe as it occurred, unavoidably, during a measurement. To mitigate this problem, a set of rectangular calibrated vessels with different areas and thickness was designed and built. The specimen volume was then estimated putting the sample in the vessel that best fitted its thickness

Table 2
Patient 1. Label of the sample, surface (A_s) and volume (V), expected activity in case of sample lesioning (A_{exp}), counts acquired and category of the sample according to the histological analysis: $SUV_{mean} = 4.3$ g/ml, expected activity on lesion during the surgery 5.4 kBq/ml.

Name	A_s [mm^2]	V [ml]	A_{exp} [kBq]	Counts [cps]	Medical report
1-A	47 ± 2	0.047 ± 0.007	0.25 ± 0.08	1.8 ± 0.2	Dura mater
1-B	19 ± 1	0.038 ± 0.003	0.20 ± 0.06	2.7 ± 0.2	Dura mater
1-C	101 ± 5	0.404 ± 0.025	2.18 ± 0.58	49.7 ± 1.0	Meningioma
1-E_3	16 ± 1	0.064 ± 0.004	0.35 ± 0.09	13.8 ± 0.5	Tumour margin
1-F_2	43 ± 2	0.171 ± 0.010	0.92 ± 0.25	20.2 ± 0.6	Meningioma

Table 3
Patient 2. Label of the sample, surface (A_s) and volume (V), expected activity in case of sample lesioning (A_{exp}), counts acquired and category of the sample according to the histological analysis: $SUV_{mean} = 3.1$ g/ml, expected activity on lesion during the surgery 3.4 kBq/ml.

Name	A_s [mm^2]	V [ml]	A_{exp} [kBq]	Counts [cps]	Medical report
2-A	60 ± 3	0.059 ± 0.009	0.20 ± 0.07	1.0 ± 0.1	Dura mater
2-B_1	108 ± 5	0.215 ± 0.019	0.73 ± 0.22	3.4 ± 0.3	Dura mater infiltrated
2-B_2	115 ± 6	0.230 ± 0.020	0.78 ± 0.24	4.6 ± 0.3	Dura mater infiltrated
2-D	56 ± 3	0.056 ± 0.008	0.19 ± 0.06	13.4 ± 0.5	Meningioma
2-E	31 ± 2	0.032 ± 0.005	0.11 ± 0.03	10.3 ± 0.5	Meningioma

without shape distortion. Since the samples were not rigid, those that slightly exceeded the vessel height were compressed to best fit. A graph paper on the vessel floor allowed redrawing its shape offline and, hence, the estimation of its volume. With this method, the probe was nearly in contact with the sample without applying pressure on it.

Finally, the specimens underwent a histopathological examination to evaluate their actual tumoural nature. No problems were present during the anatomopathological evaluation. The histological results are summarized in Tables 2–4.

2.2. The β^- probe

The core of the β^- detecting probe is a cylindrical (6 mm in diameter and 3 mm in height) scintillator, made of commercial mono-crystalline para-terphenyl doped to 0.1% in mass with diphenylbutadiene. This material turned out to be an optimal candidate for low energy electron detection [19], since it is a non–hygroscopic organic scintillator with high light yield (~2 times larger than stilbene) and low density that minimizes the sensitivity to photons.

Compared to the probe used in the first trial [18], the one used in these tests had a 1 mm larger scintillator diameter (6 mm instead of 5 mm) to increase acceptance, and a white-coloured ABS (Acrilonitrile Butadiene Stirene) ring around the scintillator to increase the light collection. Additionally, the new generation Silicon photomultiplier (SiPM SensL C-series 10035) with a lower dark current was adopted.

Fig. 1. The β^- probe prototype.

The pen like probe, shown in Fig. 1, was assembled by coupling the detector holder to an aluminium cylindrical body shielded against electromagnetic noise by a 100 μm copper sheet. On the crystal side (on the right in the picture), a 15 μm aluminium sheet ensured the light tightness of the entrance window, while the back of the probe held the connector that carried the signal. Portable electronics based on Arduino Due [20] with wireless connection to a PC or tablet was used for the read out.

The final prototype was tested in laboratory with ^{90}Sr, ^{133}Ba, ^{60}Co, ^{22}Na, ^{137}Cs sources and ad hoc phantoms activated with a ^{90}Y saline solution following the procedure described in Ref. [10]. Compared to the previous one, the new prototype significantly increased the counting rate by a factor that ranged from ~1.5 in the case of the ^{90}Y spectrum to a ~3 for 511 keV photons. The Bremsstrahlung contribution can be still considered negligible, since the probe efficiency is less than 0.1% for photons with energy below 100 keV.

2.3. Sample characterization

For an effective use of the RGS technique, it is critical to have a correct estimate of the minimum activity to be injected to detect the

Table 4
Patient 3. Label of the sample, surface (A_s) and volume (V), expected activity in case of sample lesioning (A_{exp}), counts acquired and category of the sample according to the histological analysis: $SUV_{mean} = 2.8$ g/ml, expected activity on lesion during the surgery 3.0 kBq/ml.

Name	A_s [mm^2]	V [ml]	A_{exp} [kBq]	Counts [cps]	Medical report
3-A	73 ± 4	0.146 ± 0.013	0.44 ± 0.18	1.3 ± 0.2	Dura mater
3-B	144 ± 7	0.576 ± 0.035	1.73 ± 0.70	4.6 ± 0.3	Dura mater infiltrated
3-D_1	147 ± 7	0.588 ± 0.036	1.77 ± 0.71	68.9 ± 1.2	Tumour margin
3-D_2	67 ± 3	0.268 ± 0.016	0.80 ± 0.33	42.5 ± 0.9	Tumour margin
3-D_3	44 ± 2	0.177 ± 0.011	0.53 ± 0.22	35.6 ± 0.8	Tumour margin
3-D_4	23 ± 1	0.093 ± 0.006	0.27 ± 0.11	22.3 ± 0.7	Tumour margin
3-D_5	13 ± 1	0.039 ± 0.003	0.12 ± 0.05	8.9 ± 0.4	Tumour margin
3-E_1	45 ± 2	0.136 ± 0.009	0.41 ± 0.17	10.8 ± 0.5	Meningioma
3-E_2	18 ± 1	0.055 ± 0.004	0.17 ± 0.07	4.0 ± 0.3	Meningioma
3-F_1	19 ± 1	0.075 ± 0.005	0.22 ± 0.09	10.6 ± 0.5	Tumour margin
3-F_2	17 ± 1	0.070 ± 0.004	0.21 ± 0.09	13.3 ± 0.5	Tumour margin
3-F_3	11 ± 1	0.034 ± 0.002	0.10 ± 0.04	4.1 ± 0.3	Tumour margin

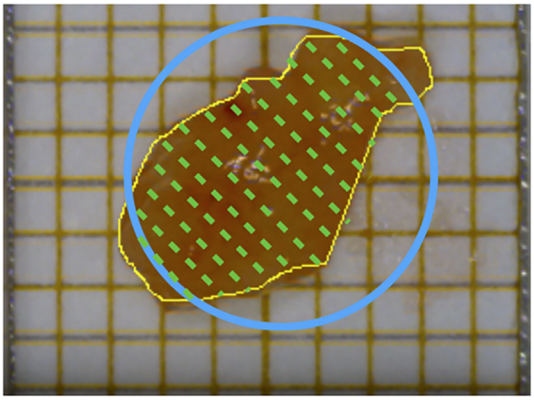

Fig. 2. Example of a photo used to estimate the specimens' area. The overlaid contour is used to estimate the sample size as explained in the text; the blue circle (d = 6 mm) shows the projection of the active area of the probe. (For interpretation of the references to colour in this figure legend, the reader is referred to the web version of this article.)

tumour remnants. To this aim, a relationship between the radioactivity of the sample and the counting rate of the device needed to be established.

The first step was, therefore, to measure the volume of each sample and to evaluate the corresponding activity.

To compute their projected area, photos of the specimens with a reference grid paper behind (see Fig. 2) were used: after a calibration between pixel and mm conducted using the grid paper, a profile of the specimen was drawn (the yellow contour line) and the corresponding area (A_s) was estimated. The figure also shows the projection of the probe tip (the blue circle): given the short penetration of the β^- particles, it was relevant to consider whether a sample was entirely contained within the probe projection or not.

The height (h) of the sample was, instead, estimated by finding in which of the boxes of fixed height (1, 2, 3 or 4 mm) it best fit.

The activity expected in the hypothesis that the specimens were all of neoplastic nature was computed by multiplying the estimated activity concentration at the time of the operation (A_{est} in Table 1) multiplied by the volume of the sample $V = A_s * h$:

$$A_{exp} = A_{est} * V \tag{2}$$

The dominant uncertainty on A_{exp} came from the fluctuations of the actual SUV within the tumour with respect to SUV_{mean}. As estimator of the spread of the SUV values over the lesion volume, we considered the standard deviation of the voxel-by-voxel value of this quantity as measured in the PET scan. To estimate the error on the calculation of the specimen volume, we assigned a 5% uncertainty to the determination of the sample area (A_s) and an error on the thickness estimation (h), computed assuming a flat distribution in a 0.5 mm range, $\sigma_h = 0.5/\sqrt{12} = 0.14$ mm.

The measured values of A_s, V and A_{exp} of every analysed specimens are reported in Tables 2–4, patient by patient.

2.4. Dosimetry and exposure measurements

The exposure of the medical personnel (nurses, surgeon, anaesthetist, anatomopathologists) was monitored. The dose delivered to the whole body were measured with AGFA Personal Monitoring dosimeters: a double-coated, low speed, high contrast X-ray film and a double-coated, very sensitive, high contrast X-ray film specifically designed for recording X-γ and β radiations. This film combination covered the measurement range from 0.1 mSv up to 1 Sv. The film-badge dosimeters were worn on the outside of clothing around the chest or torso. In addition, the surgeon and the anaesthetist were provided with an LiF thermo-luminescent dosimeter (TLD) embedded bracelet to estimate the dose to the hands. The anatomo-pathologist worn a TLD finger ring dosimeter while handling the specimens for the histological analysis.

All the surgical wastes and patient urine packs were kept in 1 cm thick methacrylate boxes, able to shield β^- emissions, and managed according to Italian radiation protection regulations.

The exposure induced by the patient and the biological samples was estimated by means of a Fluke 451B Ion Chamber Survey Meter with β radiation slide. Further, a Mini Monitor series 900 portable Geiger counter was employed for contamination measurements.

3. Results

3.1. Measured rates

The observed counting rates and the results from the specimen histology are summarized by patient in Tables 2–4, together with the estimated area, volume, and the expected activity in case of tumour. The experimental rate (in counts per second) is the mean of 5–6 measurements, each one lasting 10 s, and the statistical error is reported.

Every specimen was identified by a number and a letter. The number identified the patient; whereas the letter labelled the specimen as provided by the surgeon. To test the device sensitivity to different sizes of the sample volume and to probe the uniformity of the diffusion of the radiotracer within the lesion, some specimens were cut in several smaller samples. These sub-sections were labelled with an incremental numeric subscript.

The data was divided into two categories: dura mater and tumour (both margin and bulk) specimens. Notable differences were expected, given the different level of lesion infiltration between these categories: while the tumour tissue uptake was assumed to be the estimated SUV_{mean}, the dura mater, even if infiltrated, had a much lower uptake.

For the samples identified as meningioma, Fig. 3 shows the results in terms of dependency of the rate registered by the probe with the counts as a function of the sample volume.

For the purpose of this paper it is essential to find the quantity that correlates most to the expected activity in the lesion. Since the low penetration of electrons makes such assessment from first principles impossible, Fig. 4 shows dependence of the counting rate normalized for specimen size with the expected activity concentration (left) and dependence of the counting rate with the expected activity (right). The Pearson correlation coefficient turned out to be 0.40% and of 83% respective in the case with and without normalisation, clearing indicating that the latter option is best. To verify that such difference in correlation is significant, we allowed the rate and expected activity

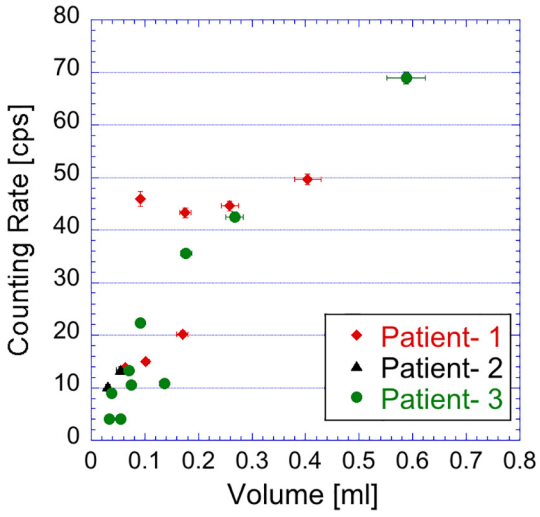

Fig. 3. Counts registered by the probe as a function of V.

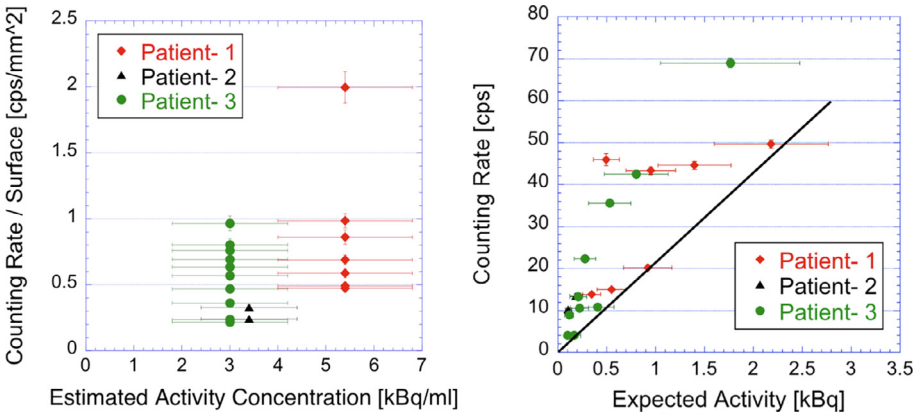

Fig. 4. Counts registered by the probe normalized by specimen size as a function of the A_{est} (left) and counting rate as a function of A_{exp} (right) for the meningioma samples. In the right plot, the superimposed line conservatively describes the relationship between the probe counting rate and the maximum expected activity that causes (Eq. (6)).

measurements to float within their errors, and obtained coefficients that average at 76% with a standard deviation of 8%.

3.2. Dose to medical personnel and patient

The readings of all personnel dosimeters (Hp(10)) were consistent with zero, meaning that the operators effective doses and the equivalent dose to hands were less than 40 μSv. Also the ambient dose equivalent (H*(10)) was negligible for all dosimeters. Nevertheless, wastes and patient urine must be properly managed as radioactive wastes, as required by Italian regulation.

Finally, the absorbed dose received by the patients was estimated using the OLINDA program, following the results in Ref. [16,21]. The more involved organs were the kidneys, spleen and urinary bladder which received an absorbed dose of 2.7, 7.0 and 2.7 mGy/MBq, respectively. Patients received the kidney protection (aminoacid solution) as used in Peptide Receptor Radionuclide therapy (PRRT) trials [14]. The contribution to the urinary bladder was reduced significantly by catheterizing the patients after the ^{90}Y-DOTATOC injection. The total effective dose was estimated to be 0.23 mSv/MBq.

4. Discussion

Considering that the counting rate the probe would measure on healthy brain of the patient for the RGS in *in vivo* status was expected to be smaller than 1 cps [18], all the samples identified by the histological exams as meningioma (bulk or margin) showed rates significantly above it, even with the smallest injected activity. The response of the detector was tested on the dura samples, as well. The signal, albeit higher than the background, was significantly lower compared to the meningioma specimens: the average signal rate in the dura is $R = 2.8 \pm 0.5$ cps, compared to the other samples for which $R = 25.2 \pm 0.8$ cps. As discussed later, this cannot be attributed to differences in volumes that in any case are on average 0.19 ml for dura and 0.33 ml in the other cases. As such, the statistical significance could not be assessed since the protocol did not include a quantification of the tumour infiltrations.

All the lesioned excised samples (bulk and margin) showed a dependence of the counting rate both on the volume V and on the total activity of the sample A_{exp}. Since electrons contributing to the measured counting rate are only those emitted by tissues within few millimetres around the probe position, a linear dependence on A_{exp} for small volumes and a saturation effect for larger samples are expected. Such correlation is nonetheless spoiled by the fact that the estimated activity (A_{est} in Eq. (2)) suffers from large uncertainties due to the fluctuations of the SUV.

4.1. Method to estimate the minimum injectable activity

The observed correlation between the measured counting rate and A_{exp} is used to determine the minimum ^{90}Y activity to be injected to get the required sensitivity to a fixed volume lesion regardless of the nature of the tumour. This minimum activity is related to the SUV_{mean} and the TNR extracted from the preoperative ^{68}Ga-DOTATOC PET of the patient.

Following the derivation in Ref. [8], for a given value of TNR the minimum average rate (R_{min}) on a tumour sample that can be identified in a measurement time of at most t_m can be estimated with a rate of false positives <1% and of false negatives <5% (see Fig. 5). To perform this calculation the relationship between the signal rate on tumour (R_{tum}) and on healthy tissue (R_{HT}) at fixed TNR must be established. From a simulation of a V = 0.1ml residual in healthy tissues, performed as described in Ref. [22], we estimated

$$R_{HT} = \frac{R_{tum}}{1 + K \times (TNR - 1)} \quad (3)$$

with $K = 0.47$. This formula takes into account that when measuring the signal on any sample intra-operatively there are contributions also from the nearby healthy tissues and that such contributions are relatively more relevant when measuring on healthy tissues. In absence of such effect, we would indeed have $K = 1$ (and $R_{HT} = R_{tum}/TNR$). The parameter K also depends on the size and shape of the sample. In the algorithm proposed here we use the parameter for a sample of the size of the minimum residual that we are interested in detecting, which is the

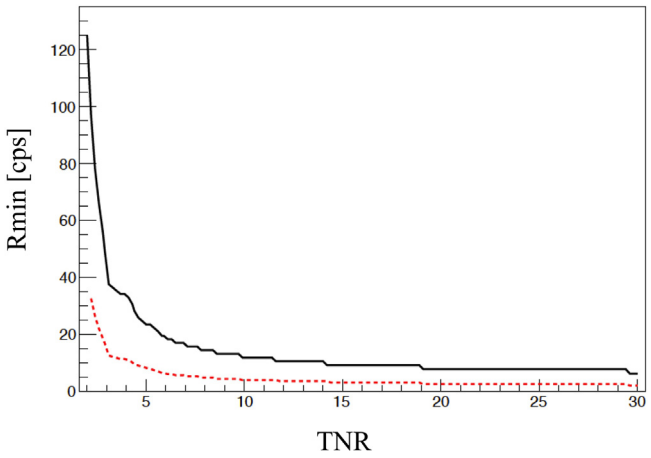

Fig. 5. Minimum counting rate as a function of the TNR of the nearby healthy tissues. The minimum counting rate is that required to observe a tumour sample in t_m = 1 s (black full line), or 3 s (dashed red line), with a rate of false positives <1% and of false negatives <5%. (For interpretation of the references to colour in this figure legend, the reader is referred to the web version of this article.)

most conservative.

Thus, given a rate on tumor, R_{tum} and assuming to integrate the signal for a time t_m, the mean number of counts is $\mu_{tum} = R_{tum} \times t_m$ on tumoral tissue and $\mu_{HT} = R_{HT} \times t_m$ on healthy tissue. Under these conditions we can estimate the false positives (*FP*) and false negatives (*FN*) rates as

$$FP = 1 - \sum_{N=0}^{th-1} \mathscr{P}_{\mu_{HT}}(N), \tag{4}$$

$$FN = \sum N = 0^{th-1} \mathscr{P}_{\mu_{tum}}(N). \tag{5}$$

where $\mathscr{P}_{\mu}(N)$ indicates the Poisson probability to have N if the mean is μ, th is the threshold on the number of counts that is supposed to be set to discriminate between tumor and healthy tissues.

It is not said that for a given value of R_{tum} at fixed t_m there exists a value of th for which $FP < 1\%$ and $FN < 5\%$. R_{min} is therefore the minimum value of R_{tum} for which this happens and therefore it represents the minimum signal rate in tumor that could be detected with a rate of false positives <1% and of false negatives <5%.

Once R_{min} is determined, (A_{min}) can be extracted from the right plot of Fig. 4. By considering, conservatively, the rightmost points in the plot (i.e. on the overlaid line) the relationship is:

$$A_{min}(\text{kBq}) = 0.043 \times R_{min}(\text{cps}). \tag{6}$$

The A_{min} can then be correlated with the minimum required per kilo administered activity of ^{90}Y, estimated at the time of the intervention[2]:

$$a_{min}^{adm} = \frac{A_{min}/V_{min}}{SUV_{mean}} \tag{7}$$

where V_{min} is the minimum volume that needs to be detected.

It should be noted that the underlying assumption is that the surface of the sample is smaller than the active area of the probe and its thickness does not exceed a few mm.

As an example, in the first meningioma patient reported in this paper: $TNR = 26$ and $SUV_{mean} = 4.3$ g/ml. If we aim at $t_m = 1$ s, then $R_{min} = 7.8$ cps and $A_{min} = 0.34$ kBq. Hence, the minimum administrable activity per kilo to identify a 0.1 ml lesion in 1 s is estimated to be $a_{min}^{adm} \sim 0.8$ MBq/kg.

Concerning the extension to other pathologies, the most favourable patient affected by high grade glioma enrolled in the feasibility study in Ref. [12] with $TNR = 9$ and $SUV_{mean} = 0.6$ g/ml may be referred to. Due to the lower SUV and TNR, t_m=3 s is set and the R_{min} is 4.4 cps. In this case, the minimum activity concentration on tumour is $A_{min} = 0.19$ kBq and the minimum administrable activity per kilo to identify a 0.1 ml lesion in 3 s is estimated to be ~3 MBq/kg, confirming the results in Ref. [12]. It is to be noted that the extension to other pathologies is reasonable because the whole algorithm is based on SUV and TNR of the lesions, regardless of the mechanisms leading to them.

5. Conclusions

One of the novelties of the RGS technique under development is the adoption of the radiotracers which are normally used in therapy for diagnostic purposes. To this aim, it is crucial to have a method to determine the minimum activity to be administered to the patients starting from their individual response to the radiotracer. The ex-vivo trials presented in this paper were, therefore, focused on this objective.

Besides the first reported patient, three new meningioma patients were injected with ^{90}Y-DOTATOC activity at the level of diagnostic purpose (~100 MBq) and then underwent surgery.

The extracted ex-vivo specimens were examined to assess the correlation between the counting rates measured by the β^- detecting probe and the administered activity.

The meningioma SUV_{mean} and the TNR ratio were estimated trough a ^{68}Ga-DOTATOC PET image of the patients. By combining this information with the dimension of the smallest residual to be detected by the actual probe, it was possible to determine a method that fixes the minimal activity to be injected. This method was tested and validated on meningioma patients using the current probe prototype and can easily be extended to any RGS applications based on radio-tracers marked with ^{90}Y.

As for the dose delivery, the injection of 1.4 MBq/kg activity corresponded to an effective dose of ~20 mSv for a 70 kg patient (which is at a level of a whole-body PET/CT examination with ^{18}F-FDG [23]) and a negligible dose to the medical personnel was confirmed.

Competing interests

F Collamati, R Faccini, and M Marafini are listed as inventors on an Italian patent application (RM2013A000053) entitled “Utilizzo di radiazione β^- per la identificazione intraoperatoria di residui tumourali e la corrispondente sonda di rivelazione” dealing with the implementation of an intra-operative β^- probe for radio-guided surgery according to the results presented in this paper. The same authors are also inventors in the PCT patent application (PCT/IT2014/000025) entitled “Intraoperative detection of tumour residues using beta- radiation and corresponding probes” covering the method and the instruments described in this paper.

This research was funded in part by Proyecto Basal FB 0821.

Ethics approval and consent to participate

All procedures performed in studies involving human participants were in accordance with the ethical standards of the institutional and/or national research committee and with the 1964 Helsinki declaration and its later amendments or comparable ethical standards. The clinical trial (EUDRACT 2013–004033-32) was approved by the Ethic Committee (institutional review board) of the *Istituto Neurologico Carlo Besta* and the *Istituto Europeo di Oncologia* of Milan. Informed consent to participate to the trial and publish individual person’s data was obtained from all patients included in the study. This article does not contain any studies with animals performed by any of the authors.

Availability of data and materials

Data on which the conclusions of the manuscript rely are presented in the tables included in the main paper.

Acknowledgments

We would like to thank G. Chiodi and L. Recchia of the electronics shop of the INFN Sez. di Roma for the hardware and software support in the realization of the probe prototypes.

References

[1] Mariani G, Giuliano AE, Radioguided Strauss HW. Surgery: a comprehensive team approach. New York: Springer; 2006.
[2] Hoffman EJ, Tornai MP, Janecek M, Patt BE, Iwanczyk JS. Intraoperative probes and imaging probes. Eur J Nucl Med 1999;26:913–35.
[3] Tsuchimochi M, Hayamaand K. Intraoperative gamma cameras for radioguided surgery: Technical characteristics, performance parameters, and clinical application. Phys Med 2013;29:126–38.
[4] Schneebaum S, Even-Sapir E, Cohen M, et al. Clinical applications of gamma-detection probes - radioguided surgery. Eur J Nucl Med 1999;26:S26–35.
[5] Riccardi L, Gabusi M, Bignotto M, et al. Assessing good operating conditions for intraoperative imaging of melanoma sentinel nodes by a portable gamma camera. Phys Med 2015;31(1):92–7.
[6] Kaviani S, Zeraatkar N, Sajedi S, et al. Design and development of a dedicated portable gamma camera system for intra-operative imaging. Phys Med 2016;32(7):889–97.
[7] Daghighian F, et al. Intraoperative beta probe: a device for detecting tissue labeled

[2] If SUV_{mean} is in g/ml, V in ml, A^{min} in kBq, then a_{adm}^{min} is in MBq/kg.

with positron or electron emitting isotopes during surgery. Med Phys 1994;21:153.
[8] Solfaroli Camillocci E, Baroni G, Bellini F, et al. A novel radioguided surgery technique exploiting β^- decays. Sci Rep 2014;4:4401.
[9] Uribe CF, Esquinas PL, Gonzalez M, Celler A. Characteristics of Bremsstrahlung emissions of ^{177}Lu, ^{188}Re, and ^{90}Y for SPECT/CT quantification in radionuclide therapy. Phys Med 2016;32:691–700. https://doi.org/10.1016/j.ejmp.2016.04.014.
[10] Russomando A, Bellini F, Bocci V, et al. An Intraoperative β^- Detecting Probe For Radio-Guided Surgery in Tumour Resection. IEEE Trans Nucl Sci 2016;63(5):2533.
[11] Collamati F, Pepe A, Bellini F, et al. Toward radioguided surgery with β^- decays: uptake of a somatostatin analogue, DOTATOC, in meningioma and high-grade glioma. J Nucl Med 2015;56:3–8.
[12] Collamati F, Bellini F, Bocci V, et al. Time evolution of DOTATOC uptake in Neuroendocrine tumours in view of a possible application of Radio-guided Surgery with β^- Decays. J Nucl Med 2015;56:1501–6.
[13] Battistoni G, Cerutti F, Fassó A, et al. The FLUKA code: description and benchmarking. AIP Conf Proc 2006;896:31–49.
[14] Bartolomei M, Bodei L, De Cicco C, et al. Peptide receptor radionuclide therapy with ^{90}Y-DOTATOC in recurrent meningioma. Eur J Nucl Med Mol Imaging 2009;36:1407–16.
[15] Heute D, Kostron H, von Guggenberg E, et al. Response of recurrent high-grade glioblastoma to treatment with ^{90}Y-DOTATOC. J Nucl Med 2010;51:397–400.
[16] Cremonesi M, Botta F, DiDia A, et al. Dosimetry for treatment with radiolabelled somatostatin analogues. A review. Q.J. Nucl. Med. Mol Imaging 2010;54:37–51.
[17] Solfaroli Camillocci E, Bocci V, Chiodi G, et al. Intraoperative probe detecting β-decays in brain tumour radio-guided surgery. Nucl Inst Met Ph Res A 2017;845:689–95.
[18] Solfaroli-Camillocci E, Schiariti M, Bocci V, et al. First ex-vivo validation of a radioguided surgery technique with β^- radiation. Phys Med 2016;32:1139–44.
[19] Angelone M, Battistoni G, Bellini F, et al. Properties of para-terphenyl as detector for alpha, beta and gamma radiation. IEEE Trans Nucl Sci 2014;61(3):1483.
[20] Bocci V, Chiodi G, Iacoangeli F, et al. The ArduSiPM a compact trasportable Software/Hardware Data Acquisition system for SiPM detector. In: 2014 IEEE Nuclear Science Symposium and Medical Imaging Conference (NSS/MIC), doi: 10.1109/NSSMIC.2014.7431252.
[21] Cremonesi M, Ferrari M, Zoboli S, et al. Biokinetics and dosimetry in patients administered with (111)In-DOTA-Tyr(3)-octreotide: implications for internal radiotherapy with (90)Y-DOTATOC. Eur J Nucl Med 1999;26(8):877–86.
[22] Mancini-Terracciano C, Donnarumma R, Bencivenga G, et al. Feasibility of the β^- radio-guided surgery with a variety of radio-nuclides of interest to nuclear medicine. Phys Med 2017;43:127–33.
[23] Brix G, Lechel U, Glatting G, et al. Radiation exposure of patients undergoing whole-body dual-modality ^{18}F-FDG PET/CT examinations. J Nucl Med 2005;46(4):608–13.